

# Microbial symbionts buffer host-plants from the demographic costs of environmental stochasticity

Joshua C. Fowler<sup>a,b,1</sup>, Shaun M. Ziegler<sup>c</sup>, Kenneth D. Whitney<sup>c</sup>, Jennifer A. Rudgers<sup>c</sup>, and Tom E.X. Miller<sup>a</sup>

This manuscript was compiled on July 31, 2023

limit = 223 out of 250 words Species' persistence in increasingly variable future climates will depend on resilience against environmental stochasticity, which tends to reduce fitness in fluctuating environments. Most organisms host microbiota that shield against stressful conditions, but deciphering how microbial symbioses buffer against the fitness costs of stochasticity requires experiments encompassing long-term environmental fluctuations. Using cool-season grasses and *Epichloë* fungal endophytes as a model system, we conducted a 14-year symbiont-removal experiment with seven host species and used experimental data to parameterize stochastic demographic models that predict the mean and variance of host fitness. We show that fungal endophytes reduce variance in the fitness of their grass hosts by 10% on average across species and that reductions of up to \*In the text you say max variance reduction is 170%. As you know, I don't really like percentages because they are easy to fudge. occur for some hosts. Hosts with "fast" life history traits that lack longevity as an intrinsic buffer experienced the greatest benefits. Under the current climate regime, contributions to host-symbiont mutualism from variance buffering were modest compared to symbiont benefits to mean fitness. However, simulations of increased environmental stochasticity amplified the benefits of variance buffering, which surpassed symbionts' mean effects that have dominated most prior research. These results establish microbial-mediated variance buffering as an important yet cryptic mechanism of resilience to increasing stochasticity under global change.

stochasticity | microbial symbiosis | demography | mutualism

Global climate change involves increases in environmental variability, including changes to precipitation patterns and the frequency of extreme weather events (1, 2). Yet, the ecological consequences of increased variability are less well understood than those of changing climate means, such as long-term warming or drying. Incorporating environmental variability into forecasts of population dynamics can improve predictions of the future.

Classic theory predicts that long-term population growth rates (equivalently, population mean fitness) will decline under increased environmental stochasticity because the costs of bad years outweigh the benefits of good years – a consequence of nonlinear averaging (3, 4). For example, in unstructured populations, the long-term stochastic growth rate in a fluctuating environment ( $\lambda_s$ ) will always be lower than the average growth rate ( $\bar{\lambda}$ ) by an amount proportional to the environmental variance ( $\sigma^2$ ):

$$\log(\lambda_s) \approx \log(\bar{\lambda}) - \frac{\sigma^2}{2\bar{\lambda}} \quad [1]$$

Populations structured by size or stage similarly experience costs of variability (5, 6). There are accordingly two pathways to increase population viability in a variable environment: increase the mean growth rate and/or dampen temporal fluctuation in growth rates, also called "variance buffering".

Both the characteristics of species and the properties of their environment can buffer demographic fluctuations, including life history traits such as longevity (7, 8), correlations among vital rates (9), transient shifts in population structure (10), the magnitude of environmental variability (11), or the degree of environmental autocorrelation (12, 13). These factors determine the risks of extinction faced by populations (14) and underlie management strategies promoting ecosystem resilience (15). Yet little is known about how biotic interactions influence demographic variability or contribute to variance buffering (16).

Most multicellular organisms host symbiotic microbes that affect growth and performance (17, 18), and many of these are transmitted via reproduction from maternal

## Significance Statement

limit = 116 out of 120 words  
Many symbiotic microbes benefit hosts under environmental stress, which is becoming more frequent in an increasingly variable climate. Using long-term field experiments with a plant-fungal endophyte model system, we show that, by limiting host exposure to environmental extremes, microbial symbionts reduce their hosts' demographic variance. Because such variance has negative fitness consequences, our results identify variance buffering a novel pathway of host-symbiont mutualism. Species with faster life histories were more strongly buffered by symbiosis, suggesting that microbial symbionts can compensate for the lack of intrinsic tolerance of variability conferred by "slow" life history traits. Increasing stochasticity magnifies the benefits of variance buffering, highlighting a key role of microbial symbionts in promoting host resilience to climate change.

Author affiliations: <sup>a</sup>Department of BioSciences, Rice University, Houston, TX, 77005; <sup>b</sup>Department of Biology, University of Miami, Miami, FL, 33146; <sup>c</sup>Department of Biology, University of New Mexico, Albuquerque, NM, 87131

J.C.F. contributed to data collection, data analysis, and led manuscript drafting. S.Z. contributed to data collection and manuscript revisions. K.D.W. contributed to research conception, data collection, and manuscript revisions. J.A.R. established transplant plots, contributed to research conception, data collection, and manuscript revisions. T.E.X.M. contributed to research conception, data collection, data analysis, and manuscript revisions.

The authors declare no conflict of interest

<sup>1</sup>To whom correspondence should be addressed. E-mail: jcf221@miami.edu

hosts to offspring (19). This process of vertical transmission links the fitness of hosts and symbionts in a feedback loop that selects for mutual benefits (20). Many vertically-transmitted microbes are mutualistic and protect hosts from stressful environmental conditions including drought, extreme temperatures, or natural enemies (21, 22). Some of the best studied examples include bacterial symbionts of aphids and other insects that provide their hosts with thermal tolerance through the production of heat-shock proteins (23), and plant-fungal symbionts that produce anti-herbivore toxins (24–26). However, these diverse protective symbioses are context-dependent: the magnitude of benefits depends on environmental conditions (27) and thus will vary temporally in a stochastic environment (28). We hypothesized that context-dependent benefits from symbionts may buffer hosts against variability through strong benefits during harsh periods and neutral or even costly outcomes during benign periods, reducing the impacts of host exposure to extremes and dampening inter-annual variance relative to non-symbiotic hosts. Variance buffering is a previously unexplored mechanism by which symbionts may benefit their hosts instead of or in addition to elevating average fitness, the focus of most previous research.

We tested the hypothesis that context-dependent benefits of symbiosis buffer hosts from the fitness costs of environmental stochasticity. We used cool-season grasses and *Epichloë* fungal endophytes as a tractable experimental model in which non-symbiotic plants can be derived from naturally symbiotic plants through heat treatment, providing a contrast of symbiont effects that controls for the confounding influence of host genetic background. *Epichloë* endophytes are specialized symbionts growing intercellularly in the aboveground tissue of ~30% of cool-season ( $C_3$ ) grass species (29). These fungi are primarily transmitted vertically from maternal plants through seeds (30). They produce a variety of alkaloids that can protect host plants from herbivory (31) and drought stress (32).

Over 14 years (2007–2021), we collected annual demographic data on the survival, growth, reproduction, and recruitment of all plants within replicated endophyte-symbiotic and endophyte-free populations at our southern Indiana field site. Through taxonomic replication (seven host-symbiont species pairs) we aimed to understand whether host life history traits could explain inter-specific variation in the magnitude of demographic buffering through symbiosis. We used the long-term demographic data to parameterize stochastic population projection models in a hierarchical Bayesian framework. Specifically, we (i) quantified the effects of symbiosis on the mean and variance of host vital rates (survival, growth and reproduction) and fitness, (ii) investigated the relationship between host life history traits and the magnitude of symbiont-mediated variance buffering, (iii) evaluated the relative contribution of mean and variance effects to the overall fitness benefits of symbiosis, and (iv) projected the consequences of symbiont-mediated variance buffering under increased environmental variability.

181  
182  
183  
184  
185  
186

## Results and Discussion

<sup>†</sup>Our experiment began in 2007 with seven grass species that host *Epichloë* fungal endophytes. Located in south-central Indiana, USA, the experiment consisted of annually censused populations founded with either naturally symbiotic plants (S+) or those that had their symbionts experimentally removed via a heat treatment (S-) (See Materials and Methods for a full list of species and experimental methods). The unique data from this long-term experiment are distinctly suitable for detecting fitness benefits of microbial symbiosis that arise through variance buffering, which on average had 13.3 individuals/m<sup>2</sup> over the course of the experiment. Each census year was a sample of inter-annual climatic variation (n = 14 years; comprising 13 demographic transition years). We fit hierarchical Bayesian generalized linear mixed models to the vital rate data using RStan (33), which allowed us to isolate endophyte effects on vital rate means and variances, borrow strength across species for some variance components, and propagate uncertainty from the individual-level vital rates to population projection models (34). The projection models were stochastic matrix population models parameterized for each host species from the vital rate regressions to quantify endophyte effects on stochastic population growth rates ( $\lambda_s$ ) and decompose the overall effect of the symbiosis into contributions through mean vital rates, variance in vital rates, and their interaction (Methods section describes the statistical methods in full).

**Quantifying symbiont mediated variance buffering.** Across seven host species, eight vital rates, 14 years, and 16,789 individual plants, our analysis provides the first empirical evidence of symbiont-mediated variance buffering. Endophytes reduced inter-annual variance for 66% (37/56) of host species-vital rate combinations (average Cohen's D for effects on vital rate standard deviation: -0.15) (Fig. 1A). Endophytes also increased mean vital rates for the majority (36/56) of host species-vital rate combos (average Cohen's D for effects on vital rate mean: 0.15), and benefits were particularly strong for host survival, plant growth and germination (Fig. 1A). The relative magnitude of symbiont effects on means versus variances differed among host species and their vital rates. For example, endophytes modestly increased mean adult survival (Fig. 1C) and reduced variance in survival (Fig. 1D) for *Festuca subverticillata*, while for *Poa alsodes*, variance buffering was more apparent in seedling growth and inflorescence production (Fig 1E). Interestingly, certain vital rates showed costs of endophyte symbiosis. Symbiotic individuals of *A. perennans* grew larger than those without endophytes (Fig. 1B), yet endophytes also reduced this species' mean germination rates (Fig. 1A). Similarly, endophyte symbiosis increased variance in seedling growth for *Elymus villosus* and *Festuca subverticillata* (Fig. 1A).

Because not all vital rates contribute equally to fitness, we used stochastic matrix models to integrate the diverse effects on vital rates described above into comprehensive measures for the mean and variance of year-to-year fitness ( $\lambda_t$ ) and the long-run fitness that integrates both mean and variance ( $\lambda_S$ ). On average across host species, endophyte-symbiotic populations had greater mean fitness (> 92% confidence that

<sup>†</sup>I would remove this paragraph here. I've moved some overview elements to the end of the Intro and other bits can be moved to the methods. I think you should get straight into results.

187  
188  
189  
190  
191  
192  
193  
194  
195  
196  
197  
198  
199  
200  
201  
202  
203  
204  
205  
206  
207  
208  
209  
210  
211  
212  
213  
214  
215  
216  
217  
218  
219  
220  
221  
222  
223  
224  
225  
226  
227  
228  
229  
230  
231  
232  
233  
234  
235  
236  
237  
238  
239  
240  
241  
242  
243  
244  
245  
246  
247  
248

249 endophytes increased  $\bar{\lambda}$ ) and lower inter-annual variability  
250 in fitness (> 86% confidence that endophytes decreased the  
251 coefficient of variation of  $\lambda_t$ ) than endophyte-free populations  
252 (Fig. 2). For some host species, the CV of  $\lambda_t$  was reduced  
253 by as much as 170% (*P. alsodes*, *F. subverticillata*), while  
254 for others, endophyte effects on variance were substantially  
255 smaller (6% lower for *E. villosus*, 16% lower for *A. perennans*),  
256 or even positive (27% increase for *E. virginicus*). When  
257 mean and variance effects of symbionts were considered  
258 together, none of the host-symbiont pairings were antagonistic  
259 (i.e., with endophytes that both decreased mean fitness and  
260 increased variance) (Fig. 2C), suggesting that variation across  
261 host species and vital rates in mean and variance effects may  
262 reflect alternative strategies that yield similar benefits of  
263 endophyte symbiosis.

264 Reduced sensitivity to drought, as has been reported for  
265 some *Epichloë* symbioses (32), is a candidate mechanism that  
266 could generate a signature of variance buffering. Accordingly,  
267 analysis of climate-explicit matrix models indicated that  
268 for five of seven taxa, symbiotic populations were less  
269 sensitive to annual or growing season drought (12-month  
270 or 3- month drought index; Standardized Precipitation-  
271 Evapotranspiration Index (35)) than symbiont-free popula-  
272 tions (Supporting Information Text; Fig. S24-S25; Table S3).  
273 However, we did not find a strong relationship between the  
274 magnitude of variance buffering and relative drought sensitivities,  
275 suggesting that other climatic factors or other temporally-  
276 varying aspects of the environment may elicit benefits of  
277 endophyte symbiosis, including documented resistance to  
278 herbivory for six host taxa (36, 37). Identifying the potentially  
279 complex relationships between vital rates and environmental  
280 drivers remains a key challenge for accurate forecasts of the  
281 ecological impacts of environmental stochasticity (38).<sup>†</sup>

282 **Life history analysis.** Long-lived species, those on the slow  
283 end of the slow-fast life history continuum, are expected to  
284 be less sensitive to environmental variability (39), a pattern  
285 which has empirical support across plants (40) and animals  
286 (8, 41). Therefore, we predicted that host species with long  
287 lifespans that produce few, large offspring would benefit less  
288 from the variance buffering effects of endophytes than species  
289 with fast life cycles that produce many smaller offspring with  
290 low per-capita chance of success (42, 43). In support of this  
291 prediction, symbionts with trait values representing faster  
292 life history strategies experienced greater variance buffering  
293 from endophytes than those with slow life histories (Fig. 3).  
294 Bayesian phylogenetic mixed-effects models, controlling for  
295 species' relatedness, indicated that variance buffering was  
296 stronger for host species with shorter lifespan (Fig. 3A; 75%  
297 probability of positive relationship with empirically observed  
298 max age) and smaller seeds (Fig. 3B; 73% probability of  
299 positive relationship with seed length). Other life history  
300 traits similarly had positive but weaker support for the  
301 prediction that faster life history traits would correlate with  
302 stronger variance buffering (Fig. S26-S28). Additionally, the  
303 three host species for which the overall mutualism was weakest  
304 (*Elymus villosus*, *Elymus virginicus*, and *Poa sylvestris*)  
305 (Fig. 2C) were the only hosts for which we observed fungal  
306 stromata, fruiting bodies capable of horizontal (contagious)  
307 transmission (Table S2), in line with theoretical expectations

311 for strict vertical transmission driving the evolution of strong  
312 host-symbiont mutualisms (20, 44). Conclusions about life  
313 histories are somewhat constrained by the narrow range of  
314 trait values among these closely related species in the grass  
315 sub-family Pooideae. Our understanding of how life history  
316 variation modulates the fitness consequences of microbial  
317 symbiosis would profit from tests across a wider span of  
318 taxonomic groups (45).

319 **Relative contributions of mean and variance effects.** To  
320 evaluate the relative importance of mean fitness benefits  
321 and variance buffering as alternative pathways of mutualism,  
322 we decomposed the overall effect of the symbiosis on  $\lambda_s$  using  
323 stochastic simulations of four versions of population models  
324 that included both mean and variance buffering effects, mean  
325 effects alone, variance effects alone, or neither mean nor  
326 variance effects. Overall, the full effect of symbiosis on  $\lambda_s$ ,  
327 averaged across host species, provided strong evidence of  
328 grass-endophyte mutualism (100% certainty of a positive  
329 total effect on  $\lambda_s$ ) (Fig. 4; see Fig. S21 for individual  
330 host species).<sup>§</sup> Contributions to this total effect derived  
331 from both mean and variance buffering effects, as well as  
332 a slightly negative interaction (i.e., the combined influence  
333 of mean and variance effects was lower than the sum of  
334 their individual effects). Endophytes' contributions to the  
335 stochastic growth rate ( $\lambda_s$ ) from mean effects were four times  
336 greater, averaged across species, than contributions from  
337 variance buffering (Fig. 4), suggesting that, under the regime  
338 of environmental variability represented by our 14-year study,  
339 damped fluctuation in fitness is a far less important element  
340 of the benefits of symbiosis than elevated mean fitness.

341 **Consequences of variance buffering under increased envi-  
342 ronmental variability.** Simulations of increased environmental  
343 variability, a key prediction of climate change forecasts (2),  
344 indicated that mutualism with microbial symbionts, and  
345 their variance buffering effects in particular, will take on  
346 increased importance for grasses in a more variable future  
347 climate. To simulate increased variability, we repeated  
348 the decomposition of  $\lambda_s$  under two additional scenarios,  
349 randomly sampling transition matrices from either the six  
350 or two most extreme years experienced by each species,  
351 subsets of the thirteen transition matrices across the study  
352 period. The six- and two-years scenarios increased the  
353 standard deviation of yearly growth rates by 1.3 and 2.1  
354 times, respectively, relative to the ambient scenario without  
355 changing mean growth rates (< 2.3% difference between  
356 simulation treatments)(See SM; Fig. S21-22). Increased  
357 variability elicited stronger mutualistic benefits of endophyte  
358 symbiosis (Fig. 3) than ambient variability (overall effect  
359 of the symbiosis increased by > 130%). This increase was  
360 driven by increased contributions from the variance buffering  
361 mechanism (from a 24% contribution in the ambient scenario  
362 to a 66% contribution in the most variable scenario). In the  
363 most variable scenario, the relative importance of mean and  
364 variance effects reverses, with variance buffering contributions  
365 that are 1.5 times greater than contributions from mean  
366 benefits, averaged across species (Fig. 4). Thus, variance  
367 buffering – a cryptic microbial influence that manifests over

368 <sup>§</sup>It would be nice if we could briefly summarize here our certainty in the total effect by species.  
369 e.g. All host species experience positive effects on  $\lambda_s$  through endophyte symbiosis and our  
370 statistical certainty of host-symbiont mutualism ranged from XX to XX%. Or something like that.

371  
372 <sup>†</sup>Could cut this sentence, it's not really saying a lot.

long temporal scales – is poised to become the dominant way in which grasses benefit from symbiosis with fungal endophytes in future climates.

Ecologists increasingly recognize the importance of symbiotic microbes for host organisms and the populations, communities, and ecosystems in which their hosts reside (46–49). Despite awareness of these ubiquitous interactions, long-term studies of microbial symbiosis are very rare. Our analysis of replicated 14-year field experiments manipulating the presence/absence of fungal symbionts in plants demonstrated for the first time that heritable microbes can commonly benefit hosts not only through improved mean fitness – the focus of most previous research – but also via buffering against environmental variance. Our results provide an important advance to improve forecasts of the responses of populations (and symbionts) to increasing environmental stochasticity under global change, suggesting that, for some species, microbial symbiosis may compensate for the lack of intrinsic tolerance of variability conferred by “slow” life history traits. We found that symbiont-mediated variance buffering made relatively weak contributions to host-symbiont mutualism under the current regime of environmental variability, but is likely to become the dominant benefit that fungal endophytes confer to grass hosts in more variable future environments. This result emerges from the context-dependent nature of grass-endophyte interactions, combined with the observation that environmental stochasticity generates fluctuation in context. These key ingredients, and thus the potential for symbiont-mediated variance buffering, similarly apply to the diverse host-microbe symbioses across the tree of life.

## Materials and Methods

**Study site and species.** This study was conducted at Indiana University’s Lilly-Dickey Woods (39.238533, -86.218150) in Brown County, Indiana, USA. This site is part of the Eastern broadleaf forests of southern Indiana, where the ranges of many understory cool-season grass species overlap. The experiment focused on seven of these grasses which host *Epichloë* endophytes (*Agrostis perennans*, *Elymus villosus*, *Elymus virginicus*, *Festuca subverticillata*, *Lolium arundinaceum*, *Poa alsodes*, and *Poa sylvestris*) (Table S1).

**Endophyte removal, plant propagation, and field set-up.** Seeds from naturally symbiotic populations of the seven focal host species were collected during summer-fall 2006 from Lilly-Dickey Woods in Brown County, Indiana, USA, and the nearby Bayles Road Teaching and Research Preserve (39.220167, -86.542683). To generate symbiotic (S+) and symbiont-free (S-) plants from the same genetic lineages, seeds from each species were disinfected with a heat treatment described in Table S1 or left untreated. The heat treatment created symbiont-free plants by warming seeds to temperatures at which the fungus becomes inviable but the host seeds can still germinate. Both heat-treated and untreated seeds were surface sterilized with bleach to remove epiphyllous microbes, cold stratified for up to 4 weeks, then germinated in a growth chamber before transfer to the greenhouse at Indiana University where they grew for ~8 weeks. We confirmed endophyte status by staining thin sections of inner leaf sheath with aniline blue and examining tissue for fungal hyphae at 200X magnification (50). We established the field plots with vegetatively propagated clones of similar sizes. By starting the experiment with plants of similar sizes and the same number of unique genotypes, we aimed to limit any potential effects of heat treatments on initial plant growth (51).

During the fall of 2007 and spring of 2008, we established 10 3x3 m. plots for *A. perennans*, *E. villosus*, *E. virginicus*, *F.*

*subverticillata*, and *L. arundinaceum* and 18 plots for *P. alsodes* and *P. sylvestris*. Half of the plots were randomly assigned to be planted with either symbiotic (S+) or with symbiont-free (S-) plants, and initiated with 20 evenly spaced S+ or S- individuals labeled with aluminum tags. In spring 2008, we placed plastic deer net fencing around each plot to limit deer herbivory and disturbance; damaged fences were regularly replaced.

**Long-term demographic data collection.** Each summer starting in 2008 through 2021, we censused all individuals in each plot for survival, growth and reproduction, adding new recruits to the census. We censused each species during its peak fruiting stage (May: *Poa alsodes*, *Poa sylvestris*; June: *Festuca subverticillata*; July: *Elymus villosus*, *Elymus virginicus*, *Lolium arundinaceum*; September: *Agrostis perennans*), such that the censuses were pre-breeding and new recruits came from the previous year’s seed production. Leaf litter was cleared out of each plot prior to the census, to aid in locating plants. For each plant remaining from the previous year, we determined survival, measured its size as a count of the number of tillers, and collected reproductive data as counts of the number of reproductive tillers and counts of the number of seed-bearing spikelets on all reproductive tillers to a maximum of three. We also tagged all unmarked individuals that were recruits from the previous years’ seed production and collected the same demographic data. New recruits typically had one tiller and were non-reproductive. In 2008 and 2009, we took additional counts of seeds per inflorescence for all reproducing individuals in the plots to ground-truth our subsample estimates. For *Agrostis perennans*, we also collected seed counts in 2010. In 2018, we stopped collecting data for the *Lolium arundinaceum* plots, which had very high survival and low recruitment, and consequently very low variation across years. For each individual in the experiment, our data record their transitions in size and reproduction from one year to the next. In total across 14 years, the dataset includes demographic information for 16,789 individual host-plants and 31,216 transition-year observations.

We expected plots to maintain their endophyte status (S+ or S-) because the fungal symbionts are almost exclusively vertically transmitted, and plots were spaced a minimum of 5 m apart, limiting seed dispersal or horizontal transmission of the symbiont between plots. However, we regularly confirmed endophyte treatment throughout the lifetime of the experiment by opportunistically taking subsets of seeds from reproductive individuals and scoring them for their endophyte status with microscopy as above. Overall, these scores reflected 98% faithfulness of recruits to their expected endophyte status across species and plots (Fig. S23; Supplement data). Additionally, we have rarely observed fungal stromata, the fruiting bodies by which *Epichloë* are potentially transmitted horizontally, provided the fly vector is also present (52). For *A. perennans*, *F. subverticillata*, *L. arundinaceum*, and *P. alsodes*, we never observed stromata. We observed stromata only infrequently for *E. villosus*, and even more rarely for *E. virginicus* and *P. sylvestris* (Table S2). For these species, stromata have only been observed on 35, 4, and 6 plants respectively, making up < 0.3% of all censused plants (Supplemental data). These stromata observations occurred irregularly across years; in most years there were no stromata during the census, and in a few years several plants produced stromata.

**Vital rate modeling.** Equipped with these demographic data, we fit statistical models for survival, growth, flowering (yes or no), fertility of flowering plants (number of flowering tillers), production of seed-bearing spikelets (number per inflorescence), the average number of seeds per spikelet, and the recruitment of seedlings from the preceding year’s seed production (Fig. S1 - S10). We fit these vital rates as generalized linear mixed models in a hierarchical Bayesian framework using RStan (33). All vital rate models included random plot and year effects, with separate estimates of year-to-year variance for symbiotic and symbiont-free plants, to quantify the effect of endophytes on inter-annual variance (Fig. S11 - S18). These variance components and other predictors as described below were given vague priors (53). We ran each vital rate model for 2500 warm-up and 2500 MCMC sampling iterations with three chains. We assessed model convergence with trace plots of posterior chains and checked for  $\hat{R}$  values less than 1.01,

497 indicating low within- and between-chain variation (54, 55). For  
 498 those models that showed poor convergence, we extended the  
 499 MCMC sampling to include 5000 warm-up and 5000 sampling  
 500 iterations, which was only necessary for seedling growth. We  
 501 graphically checked vital rate model fit with posterior predictive  
 502 checks comparing simulated data from 500 posterior draws with  
 503 the observed data (Fig. S19-S20).

504 **Survival** - We modeled survival as a Bernoulli process, where  
 505 the survival ( $S$ ) of an individual  $i$  in plot  $p$  and census year  $t$  was  
 506 predicted by the plot-level endophyte status ( $e$ ), host species ( $h$ ),  
 507 size in the preceding census, and the plant's origin status (whether  
 508 it was initially transplanted or naturally recruited into the plot).

$$S_{i,p(e),h,t} \sim \text{Bernoulli}(\hat{S}_{i,p(e),h,t}) \quad [2a]$$

$$\text{logit}(\hat{S}_{i,p(e),h,t}) = \beta_{0_h} + \beta_1 * \text{origin}_i \quad [2b]$$

$$+ \beta_{2_h} * \text{endo}_i + \beta_{3_h} * \text{size}_{i,t-1} + \tau_{e,h,t} + \rho_p \quad [2c]$$

$$\tau_{e,h,t} \sim \text{Normal}(0, \sigma_{\tau_{e,h}}^2) \quad [2d]$$

$$\rho_p \sim \text{Normal}(0, \sigma_\rho^2) \quad [2e]$$

514 Here,  $\hat{S}$  is the survival probability ( $p(e)$ ) indicates that plot  
 515 identity is uniquely associated with an endophyte status),  $\beta_{0_h}$   
 516 is an intercept specific to each host species,  $\beta_1$  is the effect of  
 517 the plant's recruitment origin,  $\beta_{2_h}$  is the endophyte effect,  $\beta_{3_h}$   
 518 is the size effect,  $\tau_{e,h,t}$  is a normally distributed year effect for  
 519 each species and endophyte status with variance  $\sigma_{\tau_{e,h}}^2$ , and  $\rho_p$  is a  
 520 normally distributed plot effect with variance  $\sigma_\rho^2$ . We assume that  
 521 origin effect  $\beta_1$  and plot-to-plot variance  $\sigma_\rho^2$  are shared across host  
 522 species, allowing us to "borrow strength" across the multi-species  
 523 dataset; other model parameters are unique to host species. We  
 524 separately modeled the survival of newly recruited seedlings, which  
 525 were typically one tiller and non-reproductive, with a similar model  
 526 but omitting size dependence and the effect of the plant's origin  
 527 status. All random effects were estimated independently between  
 528 seedling and adult vital rates models.

529 **Growth** - We modeled plant size in census year  $t$  ( $G$ ) with  
 530 the same linear predictor for the mean as described for survival.  
 531 Because we measured size as positive integer-valued counts of tillers,  
 532 we modeled it with a zero-truncated Poisson-inverse Gaussian  
 533 distribution. This distribution includes a shape parameter  $\lambda_G$  to  
 534 account for overdispersion in the data. We additionally modeled  
 535 the growth of newly recruited seedlings separately with a Poisson-  
 536 inverse Gaussian model omitting size structure and the plants'  
 537 origin status as with seedling survival.

538 **Flowering** - We modeled whether or not a plant was flowering  
 539 during the census ( $P$ ) as a Bernoulli process, with the same linear  
 540 predictor for the mean as described above for survival except that  
 541 size dependence for reproductive vital rates was determined by the  
 542 individual's size during the same census year as opposed to its size  
 543 during the previous year.

544 **Fertility** - For a plant that was flowering during the census,  
 545 its fertility was the number of reproductive tillers produced ( $F$ ),  
 546 which we modeled as a function of size in the same census period  
 547 with a zero-truncated Poisson-Inverse Gaussian distribution, with  
 548 the same linear predictor for the mean as described above.

549 **Spikelets per Inflorescence** - Spikelet production ( $K$ ) was  
 550 recorded as integer counts on up to three inflorescences per  
 551 reproducing plant. We modeled these data with a negative  
 552 binomial distribution, with the same linear predictor for the mean  
 553 as described above.

554 **Seed Production per Spikelet** - For individuals with recorded  
 555 counts of seeds production, we calculated the number of seeds per  
 556 spikelet from our counts of seeds and spikelets per inflorescence,  
 557 and then modeled seeds per spikelet ( $D$ ) as normally distributed  
 558 averages for each species and endophyte status. Because we had  
 559 less detailed data across years and plants for seed production than  
 560 for other reproductive vital rates, we omitted both plot and year  
 561 random effects.

562 **Seedling Recruitment** - We used a binomial distribution to  
 563 model the recruitment of new seedlings ( $R$ ) into the plots from  
 564 seeds produced in the preceding year, assuming no long-lived seed  
 565 bank. We included an intercept specific to each host and endophyte  
 566 status and the same random effects structure as in other models.

567 We estimated the number of seeds per plot in the preceding year  
 568 by multiplying the total number of reproductive tillers per plant  
 569 by the mean number of spikelets per inflorescence on that plant  
 570 and by a sample from the posterior distribution of mean number  
 571 of seeds per spikelet ( $D$ ). For plants with missing fertility or  
 572 spikelet data, we used the expected number of reproductive tillers  
 573 ( $F$ ) or of spikelets per inflorescence from ( $K$ ), drawing from the  
 574 full posteriors of our models. We rounded this value to get the  
 575 estimated seed production for each individual, and finally summed  
 576 across all reproductive plants in each year and plot to get the total  
 577 number of seeds produced.

578 **Stochastic population model.** Using the fitted vital rate models, we  
 579 parameterized stochastic matrix projection models including two  
 580 state variables:  $r_t$  (the number of newly recruited individuals in  
 581 year  $t$ ), and  $n_t$  (a vector including all non-seedling individuals of  
 582 sizes  $x \in \{1, 2, \dots, U\}$ , ranging from one to the maximum number  
 583 of tillers  $U$ ). We used the same model structure for each species  
 584 and endophyte status (not shown in model notation). The total  
 585 number of recruits in year  $t + 1$  is given by:

$$r_{t+1} = \sum_{x=1}^U P(x; \boldsymbol{\tau}_P) F(x; \boldsymbol{\tau}_F) K(x; \boldsymbol{\tau}_K) DR(\boldsymbol{\tau}_R) n_t^x \quad [3]$$

586 The total number of seeds produced by a maternal plant of size  
 587  $x$  is the product of the size-specific probability of flowering  $P$ ,  
 588 the number of reproductive tillers  $F$ , the number of spikelets  
 589 per inflorescence  $K$ , and the number of seeds per spikelet  $D$ .  
 590 Multiplying by the probability of transitioning from seed to seedling  
 591  $R$  gives a per-capita rate of seedling production, which is multiplied  
 592 by the number of plants of size  $x$  ( $n_t^x$ , the  $x^{\text{th}}$  element of  $n_t$ )  
 593 and summed. Each function also depends on the species- and  
 594 endophyte-specific year random effects for that vital rate ( $\boldsymbol{\tau}$ , a  
 595 vector of year-specific values derived from the statistical models).

596 Recruitment, survival and growth determine the rest of the  
 597 population dynamics of the new seedlings and larger plants. The  
 598 number of  $y$ -sized plants in year  $t + 1$  is given by:

$$n_{t+1}^y = Z(y; \boldsymbol{\tau}_Z) B(\boldsymbol{\tau}_B) r_t + \sum_{x=0}^U S(x; \boldsymbol{\tau}_S) G(x, y; \boldsymbol{\tau}_G) n_t^x \quad [4]$$

599 where  $n_{t+1}^y$  is the  $y^{\text{th}}$  element of vector  $n_{t+1}$ . The first term on  
 600 the right hand side of Eqn. 4 represents growth ( $Z$ ) and survival  
 601 ( $B$ ) of seedling recruits. The second term includes the survival  
 602 of  $x$ -sized plants and the growth of survivors from size  $x$  to  $y$ ,  
 603 summed over all  $x$ . To avoid predictions of unrealistic growth  
 604 outside of the observed size distribution, we set a ceiling on the  
 605 growth function for plants at the 97.5<sup>th</sup> percentile in the observed  
 606 size distribution (56). Each of the functions in Eqns. 3 and 4  
 607 have separate intercepts and year random effects for symbiotic and  
 608 symbiont-free populations, allowing us to calculate the effect of  
 609 endophyte symbiosis on the mean and variance of  $\lambda$ , the dominant  
 610 eigenvalue of the projection matrix. Analysis of climate-explicit  
 611 population models followed the same logic as for the climate-  
 612 implicit models presented here with the addition of parameters  
 613 defining the relationship between either annual or growing season  
 614 drought index and each vital rate. A full description of climate-  
 615 explicit methods can be found in the Supporting Information Text.

616 **Life History Analysis.** We collected metrics describing each host  
 617 species' life history to test the relationship between pace of life and  
 618 variance buffering (Table S1). Using the Rage package (57), we  
 619 calculated  $R_0$ , longevity, and generation time from our estimated  
 620 transition matrices using the S- mean matrix as the reference  
 621 condition. We recorded seed length measurements as the average  
 622 lemma length from the Flora of North America (58). We also  
 623 calculated and the 99th percentile of maximum observed age for  
 624 each species from their S- populations. Next, we fit Bayesian  
 625 phylogenetic mixed-effects models using the 'brms' package (59)  
 626 to test the relationship between each life history trait and the  
 627 estimated effect of symbiosis on the coefficient of variation from  
 628 the population model while controlling for phylogenetic non-  
 629 independence in the hosts (Fig. 26) and the symbiont (Fig.

S27). We pruned larger species-level phylogenies of plants(60) and *Epichloë* fungi (61) to include the focal species. *Agrostis perennans* was not included in the tree, and so we used a congeneric species, *A. hyemalis*. We defined separate phylogenetic covariance matrices for each pruned tree. We propagated uncertainty in the estimated variance buffering effect with a measurement error model. Thus the model for the variance buffering effect  $V$  was given by:

$$\begin{aligned} V_{MEAN,h} &\sim Normal(V_{EST,h}, V_{SD,h}) & [5a] \\ V_{EST,h} &\sim Normal(\mu_h, \sigma) & [5b] \\ \mu &= \alpha + \beta * trait + \pi & [5c] \\ \alpha &\sim Normal(0, .5) & [5d] \\ \beta &\sim Normal(0, .1) & [5e] \\ \sigma &\sim Half - Normal(.044, .01) & [5f] \\ \pi &\sim Normal(0, \sigma_\pi * \mathbf{A}) & [5g] \\ \sigma_\pi &\sim Half - Normal(0, .1) & [5h] \end{aligned}$$

Here,  $V_{EST}$  is the variance buffering effect for each host species  $h$ , estimated from the posterior mean ( $V_{MEAN}$ ) and standard deviation ( $V_{SD}$ ), propagating uncertainty associated with the effect of symbiosis in our population model. The model includes an intercept parameter ( $\alpha$ ) and a slope parameter ( $\beta$ ) defining the relationship between the variance buffering effect and the life history trait. The residual standard deviation is given by ( $\sigma$ ). We used weakly informative priors to aid model convergence. Each prior was centered at zero, except for the residual standard deviation, which we centered at the standard deviation of the estimated variance buffering effect, .04. The phylogenetic random effect ( $\pi$ ) has a standard deviation ( $\sigma_\pi$ ) which is structured by the covariance matrix  $\mathbf{A}$ . We ran each MCMC sampling chain for 8000 warmup iterations and 2000 sampling iterations. We assessed model convergence as described for the vital rate models.

**Mean-variance decomposition.** To calculate stochastic population growth rates ( $\lambda_s$ ) for each host species and endophyte status we simulated population dynamics for 1000 years by randomly sampling from the 13 annual transition matrices observed over the course of the experiment, discarding the first 100 years to minimize the influence of initial conditions. Sampling observed transition matrices produces models which realistically capture inter-annual variation by preserving correlations between vital rates (62). We tallied the total population size at each time step as  $N_t = r_t + \sum_{x=1}^U n_t^x$  and calculated the stochastic growth rate as  $\log(\lambda_s) = E[\log(\frac{N_t}{N_{t+1}})]$  (63, 64). We calculated the total effect of endophyte symbiosis as the difference in  $\lambda_s$  between S+ and

S- populations. We propagated uncertainty from the vital rate models to the calculation of  $\lambda_s$  using 500 draws from the posterior distribution of model parameters.

We decomposed the total endophyte effect on  $\lambda_s$  into contributions from effects on vital rate means, variances, and their interaction. Specifically, we repeated the calculation of  $\lambda_s$  for two additional “treatments”: (1) endophyte effects on mean vital rates only, with inter-annual variances shared between S+ and S- at the S- reference level for all vital rates, and (2) endophyte effects on vital rate variances only, with vital rate means shared between S+ and S- at the S- reference level. The combination of all four  $\lambda_s$  treatments (S+ vital rate means and variances, S- means and variances, S+ means with S- variances, S- means with S+ variances) allowed us to quantify to what extent the overall effect of symbiosis derives from changes in vital rates means, variances, and their interaction. The interaction occurs because the variance penalty to stochastic growth is proportional to the mean value of annual growth rates (see Eq. 1) such that variance is more detrimental for populations with low average growth rates. For each contribution element (variance buffering, mean effects, and their interaction), we calculated a cross species mean to assess the overall contributions (Fig. 4).

**Simulation experiment.** To create scenarios of increased variance relative to that observed during the study period, we repeated the stochastic growth rate estimation and decomposition, but sampling only a subset of the 13 observed annual transition matrices. We

created two scenarios of increased environmental variance by sampling the transition matrices associated with the six or two most extreme  $\lambda$  values, representing the six or two best and worst years, using S- populations as the reference condition. By sampling away from an average year in both directions, the mean value of annual growth rates remained similar across treatments ( $\bar{\lambda}$  averaged across species: All years = 0.71; 6 years = 0.71; 2 years = 0.73; Fig. S21A), while the standard deviation more than doubled ( $sd(\lambda)$  averaged across species: All years = 0.25; 6 years = 0.34; 2 years = 0.54; Fig. S21B), representing elevated environmental fluctuations. We performed the same mean-variance decomposition for these scenarios as for the ambient conditions (all 13 years sampled) for all host species described above (Fig. S22).

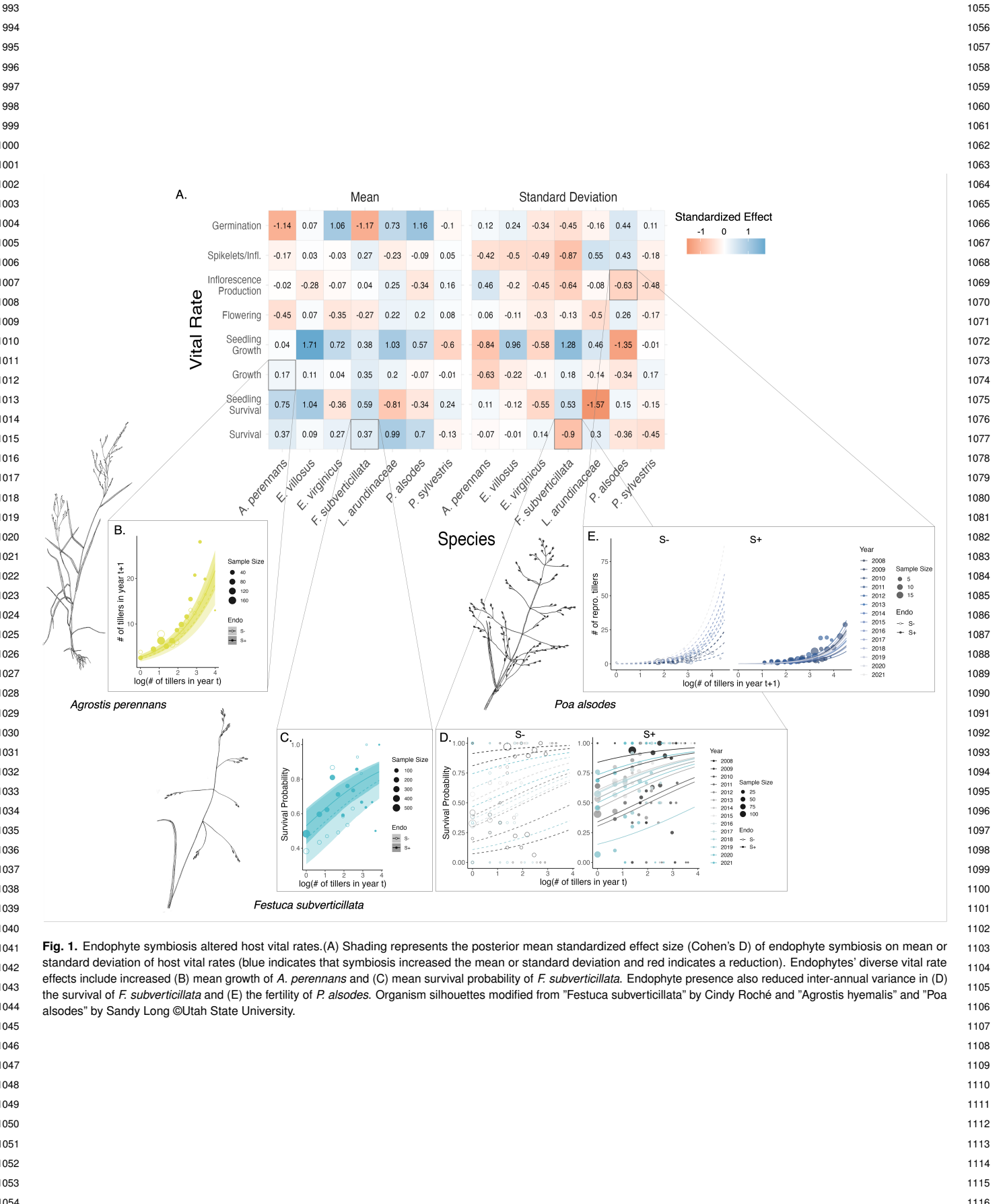
**ACKNOWLEDGMENTS.** We thank Mark Sheehan, Ali Campbell, Kyle Dickens, Blaise Willis, and Sar Lindner for contributions to field data collection. We also thank Volker Rudolf, Daniel Kowal, Lydia Beaudrot and Judie Bronstein for helpful comments on and discussion of this project. This research was supported by the National Science Foundation (Grants 1754468 and 2208857).

1. S Seneviratne, et al., *Changes in climate extremes and their impacts on the natural physical environment*. (Cambridge University Press), (2012).
2. IPCC, Climate change 2021: The physical science basis (2021).
3. RC Lewontin, D Cohen, On Population Growth in a Randomly Varying Environment. *Proc. Natl. Acad. Sci.* **62**, 1056–1060 (1969) Publisher: National Academy of Sciences Section: Biological Sciences: Zoology.
4. SD Tuljapurkar, Population dynamics in variable environments. III. Evolutionary dynamics of r-selection. *Theor. Popul. Biol.* **21**, 141–165 (1982).
5. JE Cohen, Comparative statics and stochastic dynamics of age-structured populations. *Theor. population biology* **16**, 159–171 (1979).
6. S Tuljapurkar, *Population dynamics in variable environments*. (Springer Science & Business Media) Vol. 85, (2013).
7. CA Pfister, Patterns of variance in stage-structured populations: evolutionary predictions and ecological implications. *Proc. Natl. Acad. Sci.* **95**, 213–218 (1998).
8. WF Morris, et al., Longevity can buffer plant and animal populations against changing climatic variability. *Ecology* **89**, 19–25 (2008).
9. A Compagnoni, et al., The effect of demographic correlations on the stochastic population dynamics of perennial plants. *Ecol. Monogr.* **86**, 480–494 (2016).
10. MM Ellis, EE Crone, The role of transient dynamics in stochastic population growth for nine perennial plants. *Ecology* **94**, 1681–1686 (2013).
11. RC Rodríguez-Caro, et al., The limits of demographic buffering in coping with environmental variation. *Oikos* **130**, 1346–1358 (2021).
12. S Tuljapurkar, SH Orzack, Population dynamics in variable environments i. long-run growth rates and extinction. *Theor. Popul. Biol.* **18**, 314–342 (1980).
13. J Fieberg, SP Ellner, Stochastic matrix models for conservation and management: a comparative review of methods. *Ecol. letters* **4**, 244–266 (2001).
14. ES Menges, Applications of population viability analyses in plant conservation. *Ecol. Bull.* pp. 73–84 (2000).
15. A Kuparinen, A Boit, FS Valdovinos, H Lassaux, ND Martinez, Fishing-induced life-history changes degrade and destabilize harvested ecosystems. *Sci. reports* **6**, 22245 (2016).
16. CH Hilde, et al., The Demographic Buffering Hypothesis: Evidence and Challenges. *Trends Ecol. & Evol.* **0** (2020) Publisher: Elsevier.
17. R Rodriguez, J White Jr, AE Arnold, aRa Redman, Fungal endophytes: diversity and functional roles. *New phytologist* **182**, 314–330 (2009).

- 745 37. KM Crawford, JM Land, JA Rudgers, Fungal endophytes of native grasses decrease insect  
746 herbivore preference and performance. *Oecologia* **164**, 431–444 (2010). 807
- 747 38. J Ehrlén, WF Morris, Predicting changes in the distribution and abundance of species under  
748 environmental change. *Ecol. letters* **18**, 303–314 (2015). 808
- 749 39. GI Murphy, Pattern in life history and the environment. *The Am. Nat.* **102**, 391–403 (1968). 809
- 750 40. A Compagnoni, et al., Herbaceous perennial plants with short generation time have  
751 stronger responses to climate anomalies than those with longer generation time. *Nat.  
752 communications* **12**, 1–8 (2021). 810
- 753 41. C Le Coeur, NG Yoccoz, R Salguero-Gómez, Y Vindenes, Life history adaptations to  
754 fluctuating environments: Combined effects of demographic buffering and lability. *Ecol. Lett.* 811  
755 **25**, 2107–2119 (2022). 812
- 756 42. M Rees, Evolutionary ecology of seed dormancy and seed size. *Philos. Transactions Royal  
757 Soc. London, Ser. B: Biol. Sci.* **351**, 1299–1308 (1996). 813
- 758 43. AT Moles, M Westoby, Seedling survival and seed size: a synthesis of the literature. *J. Ecol.* 814  
759 **92**, 372–383 (2004). 815
- 760 44. ME Afkhami, JA Rudgers, Symbiosis lost: imperfect vertical transmission of fungal  
761 endophytes in grasses. *The Am. Nat.* **172**, 405–416 (2008). 816
- 762 45. JM Jeschke, H Kokko, The roles of body size and phylogeny in fast and slow life histories.  
763 *Evol. Ecol.* **23**, 867–878 (2009). 817
- 764 46. ME Afkhami, SY Strauss, Native fungal endophytes suppress an exotic dominant and  
765 increase plant diversity over small and large spatial scales. *Ecology* **97**, 1159–1169 (2016). 818
- 766 47. E Smith, G Vaughan, R Ketchum, D McParland, J Burt, Symbiont community stability  
767 through severe coral bleaching in a thermally extreme lagoon. *Sci. Reports* **7**, 2428 (2017). 819
- 768 48. JW Dallas, RW Warne, Captivity and animal microbiomes: potential roles of microbiota for  
769 influencing animal conservation. *Microb. Ecol.* pp. 1–19 (2022). 820
- 770 49. L Wu, et al., Reduction of microbial diversity in grassland soil is driven by long-term climate  
771 warming. *Nat. Microbiol.* **7**, 1054–1062 (2022). 821
- 772 50. CW Bacon, JF White, Stains, media, and procedures for analyzing endophytes in  
773 *Biotechnology of endophytic fungi of grasses*. (CRC Press), pp. 47–56 (2018). 822
- 774 51. JA Rudgers, AL Swafford, Benefits of a fungal endophyte in *elymus virginicus* decline under  
775 drought stress. *Basic Appl. Ecol.* **10**, 43–51 (2009). 823
- 776 52. TL Bultman, JF White Jr, TI Bowdish, AM Welch, J Johnston, Mutualistic transfer of  
777 epichloë spermathecae by phorbia flies. *Mycologia* **87**, 182–189 (1995). 824
- 778 53. J Gabry, D Simpson, A Vehtari, M Betancourt, A Gelman, Visualization in bayesian  
779 workflow. *J. Royal Stat. Soc. Ser. A: Stat. Soc.* **182**, 389–402 (2019). 825
- 780 54. SP Brooks, A Gelman, General methods for monitoring convergence of iterative simulations.  
781 *J. computational graphical statistics* **7**, 434–455 (1998). 826
- 782 55. A Gelman, J Hill, *Data analysis using regression and multilevel/hierarchical models*.  
783 (Cambridge university press), (2006). 827
- 784 56. JL Williams, TE Miller, SP Ellner, Avoiding unintentional eviction from integral projection  
785 models. *Ecology* **93**, 2008–2014 (2012). 828
- 786 57. OR Jones, et al., Rcompadre and rage—two r packages to facilitate the use of the  
787 compadre and comadre databases and calculation of life-history traits from matrix  
788 population models. *Methods Ecol. Evol.* **13**, 770–781 (2022). 829
- 789 58. (year?). 830
- 790 59. PC Bürkner, brms: An R package for Bayesian multilevel models using Stan. *J. Stat. Softw.* 831  
791 **80**, 1–28 (2017). 832
- 792 60. AE Zanne, et al., Three keys to the radiation of angiosperms into freezing environments.  
793 *Nature* **506**, 89–92 (2014). 833
- 794 61. A Leuchtmann, CW Bacon, CL Schardl, JF White Jr, M Tadic, Nomenclatural realignment  
795 of neotyphodium species with genus epichloë. *Mycologia* **106**, 202–215 (2014). 834
- 796 62. CJE Metcalf, et al., Statistical modelling of annual variation for inference on stochastic  
797 population dynamics using integral projection models. *Methods Ecol. Evol.* **6**, 1007–1017  
798 (2015). 835
- 799 63. H Caswell, Matrix population models: Construction, analysis, and interpretation. 2nd edn  
800 sinauer associates. Inc., Sunderland, MA (2001). 836
- 801 64. M Rees, SP Ellner, Integral projection models for populations in temporally varying  
802 environments. *Ecol. Monogr.* **79**, 575–594 (2009). 837
- 803 850
- 804 851
- 805 852
- 806 853
- 807 854
- 808 855
- 809 856
- 810 857
- 811 858
- 812 859
- 813 860
- 814 861
- 815 862
- 816 863
- 817 864
- 818 865
- 819 866
- 820 867
- 821 868

**Figures**

869	931
870	932
871	933
872	934
873	935
874	936
875	937
876	938
877	939
878	940
879	941
880	942
881	943
882	944
883	945
884	946
885	947
886	948
887	949
888	950
889	951
890	952
891	953
892	954
893	955
894	956
895	957
896	958
897	959
898	960
899	961
900	962
901	963
902	964
903	965
904	966
905	967
906	968
907	969
908	970
909	971
910	972
911	973
912	974
913	975
914	976
915	977
916	978
917	979
918	980
919	981
920	982
921	983
922	984
923	985
924	986
925	987
926	988
927	989
928	990
929	991
930	992



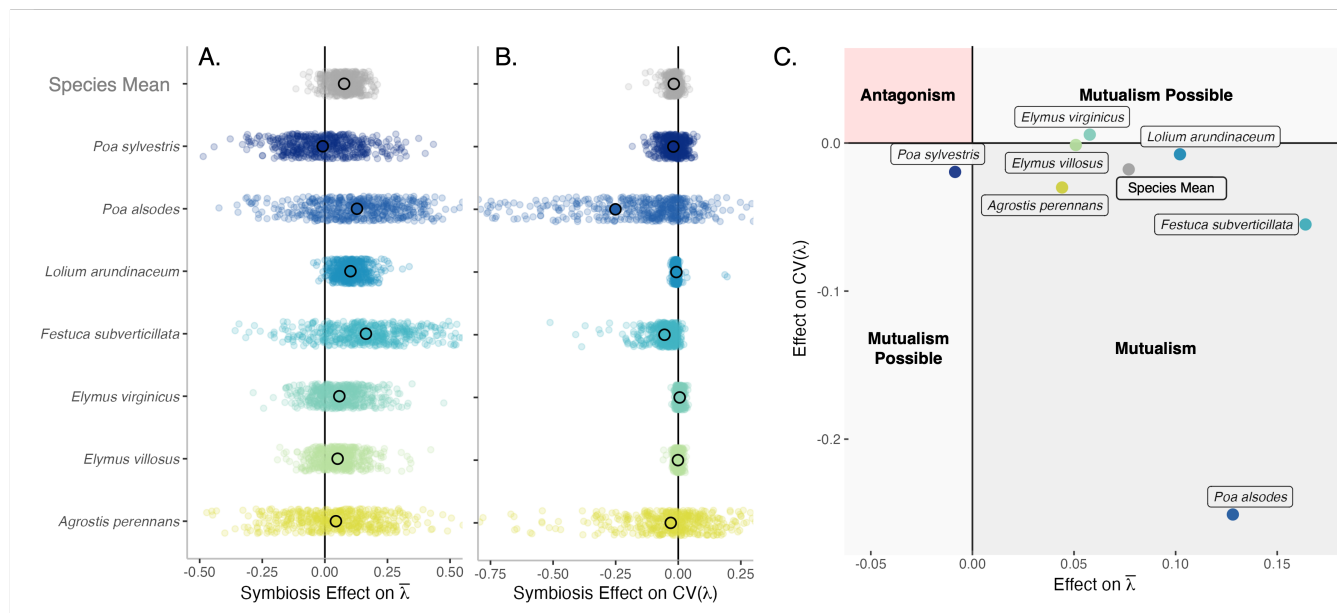


**Fig. 2.** Mean and variance-buffering effects on fitness. Black circles indicate the average effect of endophytes along with 500 posterior draws (smaller colored circles) on the (A) mean and (B) coefficient of variation in  $\lambda$  for each host species as well as a cross species mean. (C) For all hosts, endophytes either reduce variance, increase the mean, or both, and consequently when considering stochastic environments, the interactions are always at least potentially mutualistic.

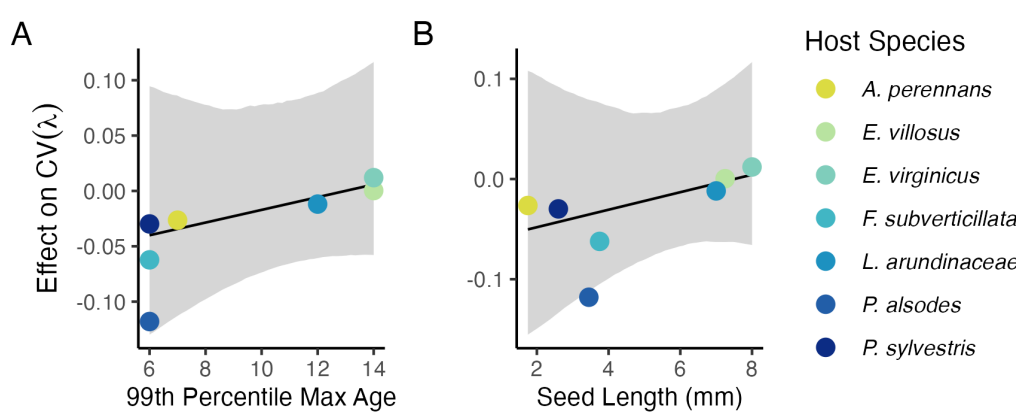


**Fig. 3.** Host species with faster life history traits experience stronger effects of symbiont-mediated variance buffering. Regressions between life history traits describing the fast-slow life history continuum ((A) 99th percentile maximum age observed during long term censuses in years; (B) Seed size) and the effect of endophyte symbiosis on the coefficient of variation in population growth rate ( $\lambda$ ). Each panel shows the fitted mean relationship (line) along with the 95% credible interval.

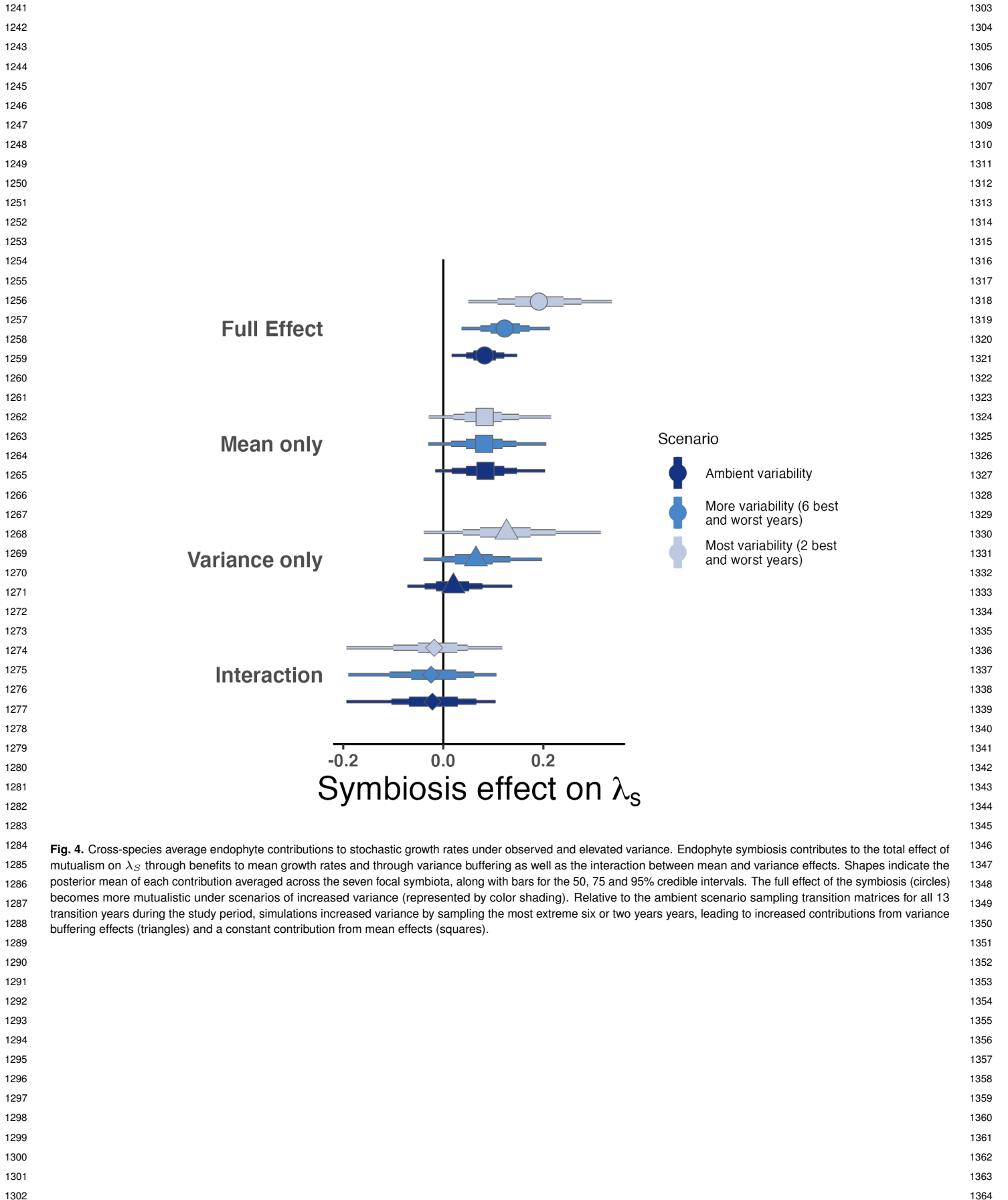


**Fig. 4.** Cross-species average endophyte contributions to stochastic growth rates under observed and elevated variance. Endophyte symbiosis contributes to the total effect of mutualism on  $\lambda_s$  through benefits to mean growth rates and through variance buffering as well as the interaction between mean and variance effects. Shapes indicate the posterior mean of each contribution averaged across the seven focal symbionts, along with bars for the 50, 75 and 95% credible intervals. The full effect of the symbiosis (circles) becomes more mutualistic under scenarios of increased variance (represented by color shading). Relative to the ambient scenario sampling transition matrices for all 13 transition years during the study period, simulations increased variance by sampling the most extreme six or two years years, leading to increased contributions from variance buffering effects (triangles) and a constant contribution from mean effects (squares).